Biofilm 9 (2025) 100259

Contents lists available at ScienceDirect

Biofilm

journal homepage: www.sciencedirect.com/journal/biofilm

A comprehensive analysis of the effect of quorum-sensing molecule 3-oxo-C12-homoserine lactone on *Candida auris* and *Candida albicans*

Fruzsina Kovács [a,b], Ágnes Jakab [a], Noémi Balla [a,b], Zoltán Tóth [a], Dávid Balázsi [a,b], Lajos Forgács [a,b], Andrea Harmath [a,b], Aliz Bozó [a], Ágota Ragyák [c], László Majoros [a], Renátó Kovács [a,*]

[a] Department of Medical Microbiology, Faculty of Medicine, University of Debrecen, Hungary
[b] Doctoral School of Pharmaceutical Sciences, University of Debrecen, 4032, Debrecen, Hungary
[c] Department of Inorganic and Analytical Chemistry, Agilent Atomic Spectroscopy Partner Laboratory, University of Debrecen, Debrecen, Hungary

ARTICLE INFO

Keywords:
Candida auris
Pseudomonas aeruginosa
In vivo
Transcriptome
Homoserine lactone
Iron

ABSTRACT

Candida auris occupies similar niches in various infections as *Pseudomonas aeruginosa*; however, the details of their interspecies communication remain largely unknown. To gain deeper insights into this relationship, phenotypic and transcriptomic analyses were conducted in the presence of the primary *P. aeruginosa* quorum-sensing molecule, N-(3-oxododecanoyl)-L-homoserine lactone (HSL), against *C. auris*, with the results compared to those of *C. albicans*. Our findings indicate that HSL-induced effects are not specific to *C. albicans*; additionally, several characteristics are present in *C. auris* but not in *C. albicans* following HSL exposure. Significant HSL-induced reduction was observed in growth and adhesion of *C. auris* cells in time -and concentration-dependent way ($p < 0.01$-0.001). Moreover, HSL reduced intracellular iron and zinc levels ($p < 0.05$-0.001); furthermore, it modulated *C. auris* metabolism toward beta-oxidation, which may be associated with the observed reduction in *in vivo* virulence at lower HSL concentrations compared with *C. albicans*. RNA-sequencing transcriptome analysis of *C. auris* revealed 67 and 306 upregulated genes, as well as 111 and 168 downregulated genes, in response to 100 and 200-μM HSL, respectively. We identified 45 overlapping upregulated and 25 overlapping downregulated genes between the two HSL concentrations. Similar to other *Candida*-derived C12 compounds (e.g., farnesol), HSL reduces several *C. auris* survival strategies, which may significantly influence the nature of *P. aeruginosa*–*C. auris* co-habitation. In conclusion, the obtained findings on *C. auris* do not provide clear evidence that HSL mediated effects have any favourable consequences in terms of *P. aeruginosa*-*C. auris* co-colonisation and/or co-infections.

1. Introduction

Bacterial–Candidal polymicrobial infections and related microbial interactions are commonly observed in clinical practice, particularly in intensive care units, where they are associated with high incidence of mortality and morbidity due to their increased dissemination and the lack of effective therapeutic algorithms. Despite their significance, few of these interactions have been thoroughly characterised at the molecular or physiological level [1–3]. The outcome of these polymicrobial infections are attributes not only by the composition of causative microbial population, but also by the nature of bacterial-fungal communications. These communications are often linked to quorum-sensing molecules, which significantly affect microbial growth, morphology, and virulence [4,5]. *Pseudomonas aeruginosa* and various *Candida* species are generally benign members of the human microbiome; however, they can be co-isolated from clinical samples, such as wound, soft tissue infections and in cystic fibrosis [6].

Previous studies have identified N-(3-oxododecanoyl)-L-homoserine lactone (HSL) as a primary quorum-sensing molecule in *P. aeruginosa*. This molecule plays a crucial role in regulating bacterial virulence factor production and has been shown to inhibit hyphal development, reduce biofilm formation, and induce apoptosis in *Candida albicans* [6,7]. However, these HSL mediated effects on *C. albicans* cannot necessarily be extrapolated to non-albicans *Candida* species, as indicated by several

This article is part of a special issue entitled: Eurobiofilms 2024 published in Biofilm.

* Corresponding author. Department of Medical Microbiology, Faculty of Medicine, University of Debrecen, Nagyerdei krt. 98., 4032, Debrecen, Hungary.
E-mail address: kovacs.renato@med.unideb.hu (R. Kovács).

https://doi.org/10.1016/j.bioflm.2025.100259
Received 15 October 2024; Received in revised form 8 January 2025; Accepted 28 January 2025
Available online 30 January 2025

studies [8–10].

Unlike most other *Candida* species, *C. auris* efficiently colonises the skin and can contaminate the patient's environment, contributing to healthcare-associated outbreaks [11]. Interestingly, patients without *C. auris* colonisation mainly harbour commensal bacteria dominated by Gram-positive species [11]. By contrast, *C. auris*-positive patients exhibit a distinct bacterial skin community, predominantly containing Gram-negative bacteria, including *P. aeruginosa* [12,13]. Despite this frequently observed association, there is a significant lack of data on whether *P. aeruginosa* influences *C. auris* physiological properties or *P. aeruginosa*-derived quorum-sensing molecule HSL interacts with *C. auris*, even though they might share the same ecological niche in clinical settings. There is no solid evidence that HSL mediated signalling interactions have any effect on *P. aeruginosa-C. auris* co-colonisation and/or co-infections.

Hence, in this study, we performed a detailed physiological and molecular characterisation of the effects of HSL on *C. auris* and compared these findings to those obtained for *C. albicans* as well documented reference species in *Candida-Pseudomonas* co-culture-based investigations.

2. Materials and methods

2.1. Isolates and culture conditions

The reference strains *C. albicans* SC5314 and *C. auris* NCPF 8973, which are derived from the South Asian/Indian lineage, were used in this study. Both strains were maintained on yeast peptone dextrose (YPD) agar plates [composed of YPD broth (1 % yeast extract, 2 % peptone, 2 % glucose) and 2 % agar, pH 5.8 (VWR, Debrecen, Hungary)] at 37 °C. HSL was obtained from Merck (Budapest, Hungary) as a 50-mM stock solution in dimethyl sulfoxide (DMSO) (VWR, Debrecen, Hungary). An equal volume of DMSO was used in all control samples, with the final solvent concentration maintained at ≤1 % (v/v). Working concentrations of HSL were prepared in YPD. For *in vitro* experiments, HSL concentrations of 100 and 200-μM were tested, while *in vivo* experiments included an additional concentration of 50-μM [14].

2.2. Planktonic growth conditions

Candida auris and *C. albicans* strains were pre-cultured in YPD broth overnight at 37 °C and then diluted to an optical density at 640 nm (OD_{640}) value of 0.1 in YPD broth (20-mL aliquots in 100-mL Erlenmeyer flasks). Cultures were incubated at 37 °C with shaking at 140 rpm for 6 h. HSL (at a final concentration of 100 or 200-μM) was added after 4 h of incubation, during the exponential growth phase. Control flasks without HSL contained 1 % DMSO. *Candida* growth was monitored at 1-h intervals by measuring cell density through absorbance readings at 640 nm and by determining the dry cell mass (DCM) [9,10].

2.3. Initial adhesion and early biofilm forming ability of Candida cells in the presence and absence of HSL

To assess the metabolic activity of adhered *Candida* cells, fungal isolates were suspended in YPD broth at a concentration of 1×10^6 cells/mL, and 100-μL aliquots were inoculated into flat-bottom 96-well sterile microtiter plates (TPP, Trasadingen, Switzerland). The plates were statically incubated at 35 °C, with pre-determined wells assigned as endpoints at 2, 4, 6, and 8 h. Different concentrations of HSL were added to all wells in YPD at time zero, simultaneously with the fungal cells [10,15]. Following incubation for 2, 4, 6, or 8 h, the corresponding wells were washed with sterile physiological saline, and the metabolic activity of the adhered cells was measured using the [2,3-bis (2-methoxy-4-nitro-5-sulfophenyl)-2H-tetrazolium-5-carboxanilide] (XTT) reduction assay [16].

Baseline metabolic activity was defined as 100 %, corresponding to the value measured in untreated cells at each respective time point. Three independent experiments were conducted, and the mean OD_{492} values obtained were reported with the standard deviation.

These metabolic activity-based experiments were supplemented with widefield fluorescence microscopy. The adhesion of *C. auris* and *C. albicans* was examined on the surface of 8-well Permanox slides under static conditions at 37 °C for 24 h (Lab-Tek® Chamber Slide™ System; VWR, Debrecen, Hungary) [17]. As described in the previous experiments, chambers were assigned to endpoints at 2, 4, 6, and 8 h, with different HSL concentrations added in YPD at time zero alongside the fungal cells. After incubation for the specified durations, the chambers were washed with sterile physiological saline, and the adhered cells were stained with 20 μL of 3-mg/mL Calcofluor-white (Thermo Fisher Scientific, Waltham, MA, USA) [17]. Calcofluor-white binds indiscriminately to the chitin content of the fungal cell wall [18]. The fluorescently stained cells were further incubated at 37 °C for 30 min, after which 10 μL of medium was mounted on a slide and examined using a Zeiss Axioskop 2 MOT microscope equipped with a Zeiss Axiocam HRc camera to assess cell morphology [17]. Image acquisition was performed using Zeiss Axiovision 4.8.2 software.

2.4. Effect of HSL on virulence of Candida species

BALB/c immunocompromised female mice (21–23 g) (Charles River Laboratories, Wilmington, MA, USA) were used to assess the effect of HSL exposure on the virulence of *C. auris* compared with *C. albicans*. The animals were maintained in accordance with the Guidelines for the Care and Use of Laboratory Animals, and all experiments were approved by the Animal Care Committee of the University of Debrecen, Debrecen, Hungary (permission no. 12/2014 DEMÁB and 8/2024 DEMÁB). Mice were immunosuppressed using intraperitoneal cyclophosphamide, administered as follows: 4 days prior to infection (150 mg/kg of body weight), 1 day prior to infection (100 mg/kg), 2 days postinfection (100 mg/kg), and 5 days postinfection (100 mg/kg) [8,9].

Mice were inoculated intravenously via the lateral tail vein with an infectious dose of 8×10^6 and 2×10^4 CFU/mouse for *C. auris* and *C. albicans*, respectively [8,9]. Intraperitoneal treatment with 50, 100 and 200-μM HSL (0.5 mL in physiological saline) was initiated 24 h post-inoculation and continued for 5 days (approximately 0.35, 0.70 and 1.40 mg/kg of body weight, respectively). Control mice received 0.5 mL of sterile physiological saline. Although HSL may cause toxic effect and induce apoptosis, these harmful consequences are known to be concentration-dependent and cell line-specific [19]. Administration of 15 and 25 mg/kg/day HSL inhibits Lewis lung carcinoma tumor growth and induces tumor cell apoptosis *in vivo* in 8-week-old C57BL/6 mice in a dose-dependent manner [20]. In BALB/c mice 20 mg/kg HSL treatment led to systemic inflammation by disrupting intestinal barrier function [21]. Sensitivity to HSL varies between cell lines; for instance, intestinal goblet cells (LS174T) are significantly more sensitive to HSL than are HCT116 cells, highlighting its cell-specific effects [22].

On day 6 post-infection, all mice were euthanised by cervical dislocation, and their kidneys were removed, weighed, and aseptically homogenised. Homogenates were serially diluted 10-fold, and 100-μL aliquots of both the undiluted and diluted homogenates were plated onto Sabouraud dextrose agar plates, followed by incubation at 37 °C for 48 h [8,9].

Kidneys from both treated and untreated mice were subjected to histological analysis. Histopathological examination and histochemical staining were performed on routine formalin-fixed, paraffin-embedded mouse kidney tissues. Serial 4-μm-thick sections were cut from the paraffin blocks, and periodic acid–Schiff staining was performed [8,9,23].

2.5. Determination of intracellular metal contents of Candida cells

After 4 h of exposure to HSL, the intracellular metal contents (iron,

zinc, copper, and manganese) of the dry biomass were measured using inductively coupled plasma optical emission spectrometry (Agilent Technologies, Santa Clara, CA, USA), as previously described [10,24]. Briefly, lyophilised samples were weighed into glass beakers using an analytical balance (Precisa ES 225SM-DR) and then digested through atmospheric wet digestion with a mixture of 3 mL of 65 % (m/m) HNO_3 (reagent grade; Merck, Budapest, Hungary) and 1 mL of 30 % (m/m) H_2O_2 (reagent grade; Merck, Budapest, Hungary) [10,24].

The digested samples were then transferred into volume-calibrated plastic centrifuge tubes without any loss and diluted to a final volume of 12 mL using 0.1 M HNO_3 prepared in ultrapure water (Synergy UV; Merck, Budapest, Hungary). The solutions were stored at room temperature before undergoing further elemental analysis by inductively coupled plasma optical emission spectrometry. The intracellular metal contents of the samples were calculated in terms of DCM units (mg/kg) and were determined in triplicate, with mean ± standard deviation values reported [10,24].

2.6. High-throughput RNA sequencing (RNA-seq)

Total transcriptome sequencing was conducted to identify the molecular events in *C. auris* and *C. albicans* that are significantly altered in the presence of 100 or 200-μM HSL. A comprehensive comparison of gene transcription profiles was performed to evaluate the impact of these HSL concentrations on each species. Differentially expressed genes (DEGs) were analysed for each treatment relative to the solvent control, as well as between the two species at the given concentrations, to identify significant upregulation or downregulation of genes across the various groups.

2.7. RNA extraction

Samples were collected after 2 h of exposure to HSL and then washed three times with physiological saline. Total RNA was isolated from lyophilised fungal cells according to the method published by Chomczynski [25], and DNA was digested using a DNase I kit (Merck, Budapest, Hungary) following the manufacturer's instructions. The final RNA concentration and quality were determined using a NanoDrop 2000 (Thermo Fisher Scientific, Waltham, MA, USA) and an Agilent Bio-Analyzer (Agilent Technologies, Santa Clara, CA, USA), according to the manufacturer's protocol. Three-three biological replicate control samples were used for RNA-seq measurements in each concentration for *C. albicans* and *C. auris*.

2.8. Quantitative reverse-transcription polymerase chain reaction (RT-qPCR)

The Luna Universal One-Step RT-qPCR Kit (New England Biolabs, Ipswich, MA, USA) was used for RT-qPCR assays, following the manufacturer's protocols. Each reaction contained 500 ng of DNase-treated total RNA and oligonucleotide primer pairs listed in Table S1. Gene expression was determined using a LightCycler 480 II real-time PCR instrument (Roche, Basel, Switzerland). Relative gene expression values were calculated using the ΔCP method (difference between the crossing point of the reference and target genes within a sample), with the *C. albicans* (C1_13700WA) and *C. auris* (B9J08_000486) actin genes serving as endogenous controls (Table S1).

2.9. RNA sequencing

Construction of the cDNA library, RNA-seq, and data analysis were conducted by the Genomic Medicine and Bioinformatic Core Facility, Department of Biochemistry and Molecular Biology, Faculty of Medicine, University of Debrecen, Hungary, as described in detail by Jakab et al. [24]. cDNA libraries were prepared from 0.25 μg of high-quality total RNA using the NEBNext RNA Sample Preparation kit (New England Biolabs, Ipswich, MA, USA) and validated according to the manufacturer's protocol. Sequencing was performed using the Illumina NextSeq 500 platform (Illumina, San Diego, CA, USA) to generate single reads of 75 bp in length. For *C. albicans* and *C. auris* samples, approximately 22.5–31.4 million and 18.6 to 23.1 million reads per sample were generated, respectively.

The quality of the raw sequences was assessed using the FastQC package (www.bioinformatics.babraham.ac.uk/projects/). Raw reads were aligned to the reference genomes of *C. albicans* strain SC5314 and *C. auris* strain B8441 with the HISAT2 v2.1 aligner, in combination with SAMtools. The reference genome for *C. albicans* (GCF_000182965.3) was accessed from the NCBI database at https://www.ncbi.nlm.nih.gov/datasets/genome/GCF_000182965.3/on November 30, 2023, and the reference genome for *C. auris* (GCA_002759435.2) was accessed at https://www.ncbi.nlm.nih.gov/datasets/genome/GCA_002759435.2 on the same date. HISAT2 was used with default parameters, which settings are available at the following website: http://daehwankimlab.github.io/hisat2/. These default settings are appropriate for low quality reads and adapter sequences. BAM files were generated, with ≥94 % of the raw reads successfully aligned to the *C. albicans* genome and ≥93 % to the *C. auris* genome.

Further downstream analysis was performed using StrandNGS v4.0 software. Raw (FASTQ, FASTA) and pre-aligned (BAM, SAM) data were imported for analysis. The workflow consists of the following steps: (i) quantification; (ii) normalization; (iii) statistical test for determining differential expression: *t*-tests, Mann-Whitney, and analysis of variance for identifying differentially expressed genes under various experimental conditions. The software-integrated DESeq algorithm was used to obtain normalized gene expression values. Afterwards, these values were used for determining the differentially expressed genes between experimental conditions by moderated *t*-test with the Benjamini–Hochberg false discovery rate for multiple testing correction. We compared the averaged normalized gene expression values of control vs. 100-μM HSL treated, control vs. 200-μM HSL treated and 100-μM HSL treated vs. 200-μM HSL treated groups, respectively. R^2 values show the variance between the compared groups (Fig. S1, Table S3).

Upregulated and downregulated genes were identified as DEGs (corrected *p*-value of <0.05) based on their fold change (>1.5 or <-1.5).

2.10. Gene set enrichment analysis

The Candida Genome Database Gene Ontology Term Finder (http://www.candidagenome.org/cgi-bin/GO/goTermFinder) and FungiDB (https://fungidb.org/fungidb/app/) platforms, using default settings, were employed to characterise the upregulated and downregulated sets of DEGs. Only hits with a corrected *p*-value <0.05 were considered during the evaluation process (Table S2).

2.11. Statistical analysis

Growth experiments and intracellular metal content determination were performed in triplicate, and the mean ± standard deviation was calculated. Statistical comparisons between treated and untreated data were carried out using a paired Student's *t*-test with GraphPad Prism 10.2.3 software. Differences between treated and control cells were considered significant if the *p*-value was <0.05. Regarding *in vivo* experiments, the kidney tissue burden was analysed using a Kruskal–Wallis test with Dunn's post-test (GraphPad Prism 10.2.3). A *p*-value of <0.05 was considered statistically significant.

3. Results

3.1. Planktonic growth was inhibited by HSL treatment

The growth of *C. auris* and *C. albicans* was examined following

treatment with 100 and 200-μM HSL in YPD broth (Fig. 1). Adding HSL to precultured *Candida* cells resulted in significant growth inhibition beginning 2 h post-exposure, as confirmed by absorbance measurements (OD_{640}) and DCM determination. For *C. auris*, the absorbance values at OD_{640} were 1.06 ± 0.03 for the untreated control, 0.97 ± 0.02 for the 100-μM-treated cells, and 0.82 ± 0.01 for the 200-μM-exposed cells ($p <$ 0.001–0.01) (Fig. 1A). The corresponding DCM values were 0.26 ± 0.02 g/L for the untreated control, 0.13 ± 0.02 g/L for the 100-μM-treated cells, and 0.09 ± 0.02 g/L for the 200-μM-exposed cells ($p < 0.001$).

For *C. albicans*, only the 200-μM treatment had a significant effect at 2 h post-exposure with absorbance measurements of 1.33 ± 0.04 and 1.24 ± 0.03 for the untreated control and 200-μM-exposed cells, respectively ($p < 0.01$) (Fig. 1B). The DCM values were 0.54 ± 0.03 and 0.46 ± 0.02 for the untreated control and 200-μM-exposed cells, respectively) ($p < 0.01$).

3.2. Adhesion is negatively influenced by HSL exposure

HSL exposure had a concentration-independent effect on the metabolic activity of adhered *C. auris* cells, while a concentration-dependent effect was observed for *C. albicans* (Fig. 2A and B). After 8 h of exposure, the metabolic activity of adhered *C. auris* cells was 64.8 % ± 2.5 % and 61.4 % ± 8.4 % for the 100- and 200-μM HSL treatments, respectively, compared with the untreated control. By contrast, *C. albicans* cells exhibited 78.5 % ± 4.3 % and 55.4 % ± 6.4 % metabolic activity for the 100- and 200-μM HSL treatments, respectively, compared with control cells (Fig. 2A and B).

Unlike *C. auris*, the lowest metabolic activity of *C. albicans* was observed at 6 h, with values of 65.4 % ± 6.0 % for the 100-μM treatment and 39.3 % ± 2.8 % for the 200-μM treatment. At 8 h, an increase in metabolic activity was detected in *C. albicans* cells, whereas *C. auris* cultures were further suppressed by HSL exposure (Fig. 2A and B). These results were consistent with the observed fluorescent images. HSL treatment significantly inhibited the proliferation of both *Candida* species compared with the control. At 8 h, large aggregates (30–50 cells) were observed for *C. auris*. Interestingly, HSL could not completely inhibit germ tube or hyphae/pseudohyphae formation for *C. albicans*. However, the filamentous forms were disorganised, with extensive hyphae aggregations observed following 8 h of exposure to 100 or 200-μM HSL (Fig. 2A and B).

3.3. Effect of HSL on virulence of Candida species in systemic mouse model

The results of the *in vivo* experiments are shown in Fig. 3A and B for *C. auris* and *C. albicans*, respectively. For *C. albicans*, all treatment arms resulted in statistically comparable kidney fungal burdens compared with the untreated control (Fig. 3B). Notably, HSL concentrations of 50 and 100-μM significantly decreased the number of viable *C. auris* cells compared with the untreated control (Fig. 3A). The histopathology results were consistent with the fungal burden findings. In untreated control mice, *C. auris* produced extensive lesions, with both single and numerous budding yeast cells. Daily treatment with 50-μM HSL markedly reduced the number and severity of these lesions (Fig. 3A).

By contrast, all treatment arms caused multiple extended fungal lesions in the kidney tissue of mice infected with *C. albicans*. These lesions were characterised by the presence of single and budding yeast cells, as well as pseudohyphae and hyphae, in all groups (Fig. 3B).

3.4. Transcriptome response of C. albicans to HSL

Exposure to 200-μM HSL induced a more extensive transcriptome change in *C. albicans* than the 100-μM HSL treatment (Fig. 4A). The number of upregulated and downregulated genes was 189 and 132 for 100-μM HSL and 354 and 540 genes for 200-μM HSL, respectively, compared with the untreated controls (Fig. 4A). Interestingly, there was minimal overlap in the DEGs between the two concentrations, with only 44 upregulated and 76 downregulated genes shared between them (Fig. 4B). Approximately half of the genes with increased (310 genes) or decreased (464 genes) transcription was observed exclusively in response to the 200-μM HSL exposure compared to the 100-μM HSL treatment (Fig. 4B). For the eight genes selected for RT-qPCR (Table S1), the transcriptional activities determined with RT-qPCR showed a strong correlation with the RNA-seq data (Pearson's correlation coefficient: 0.91–0.95) (Table S1).

The upregulated and downregulated gene sets were characterised using the Candida Genome Database and FungiDB gene set enrichment analyses (Table 1 and S2). According to these data, processes related to vegetative growth were downregulated, including the mitotic cell cycle (54 genes), DNA replication (32 genes), RNA metabolic processes (139 genes), ribosome biogenesis (136 genes), translation (125 genes), sterol

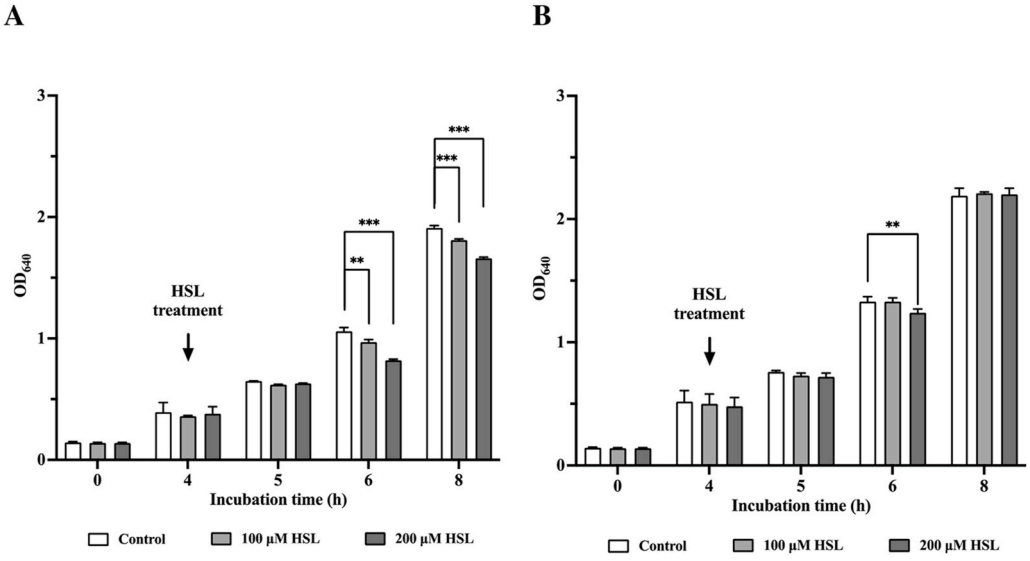

Fig. 1. 3-oxo-C12-homoserine lactone (HSL) exposure inhibits the growth of *Candida auris* (A) and *C. albicans* (B). Changes in the growth of *Candida* cells were monitored by measurement of the absorbance (OD_{640}). Following a 4-h incubation time, HSL was added at a final concentration of 100 and 200-μM to the YPD cultures. The asterisks indicate a statistically significant difference between control and HSL-treated cultures calculated by paired Student's *t*-test (***, $p < 0.001$; **, $p < 0.01$).

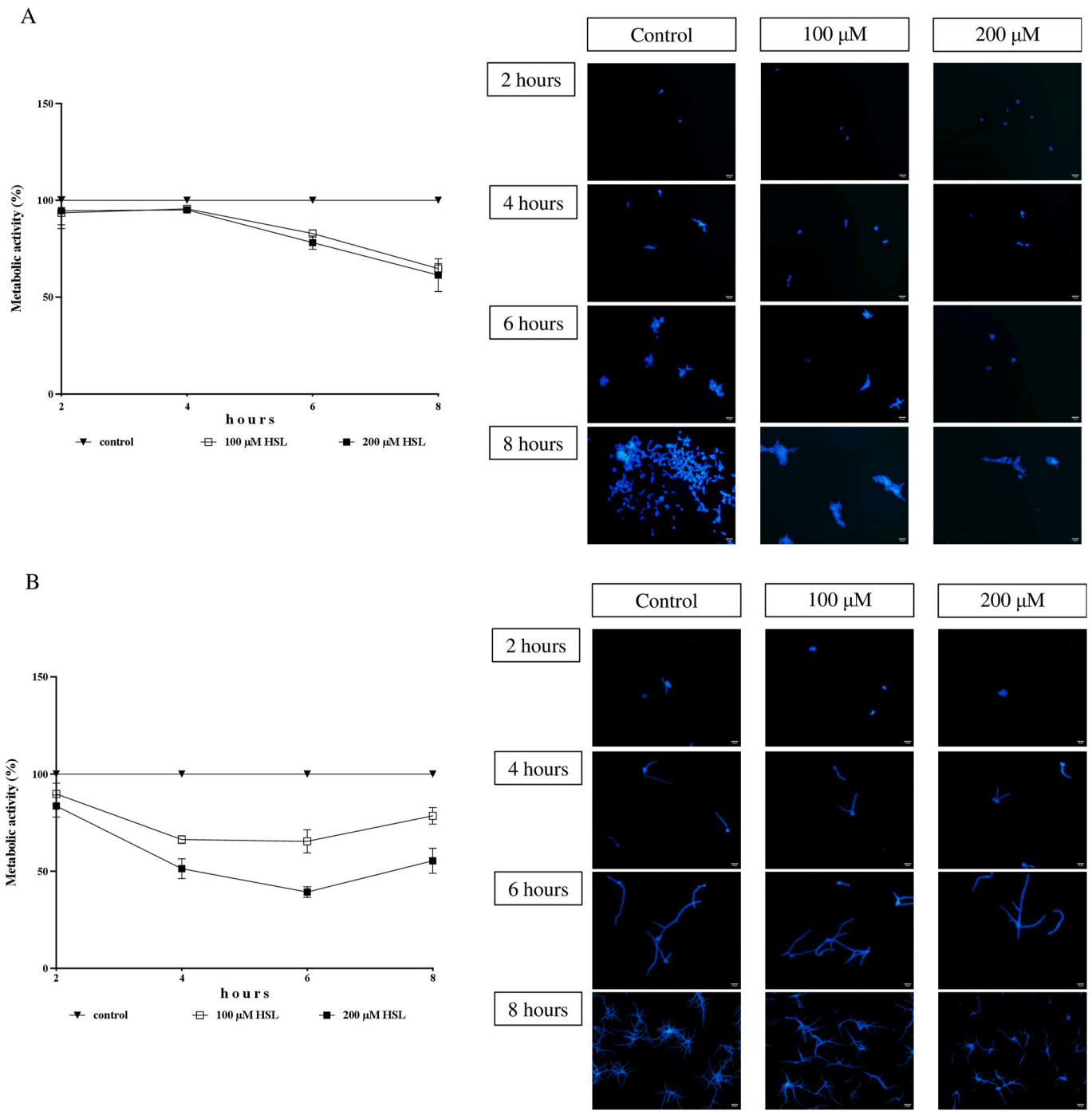

Fig. 2. Metabolic activity changes over time in case of adhesion in the presence of given 3-oxo-C12-homoserine lactone (HSL) concentrations (100 and 200-µM) for *Candida auris* (A) and *C. albicans* (C), respectively. Relative metabolic activity values (%) are presented where control baseline metabolic activity was defined as 100 %, corresponding to the value measured in untreated cells at each respective time point. Each time-point represents mean ± SD (standard deviation) of metabolic activity of isolates (three independent experiments per isolate). Calcofluor-white based fluorescence microscopy images of *C. auris* (B) and *C. albicans* (D) cells at 2, 4, 6 and 8 h (B). Bars, 10-µm.

biosynthesis (32 genes; e.g., *HMG1*, *IDI1*, *CYB5*, *ERG1*, *ERG3*, *ERG6*, *ERG9*, *ERG11*, *ERG12*, *ERG13*), and fatty acid biosynthesis (e.g., *FEN12*, *FEN1*, *FAD3*, *EHT1*, *ERG3*, *SUR2*, *ERG251*, *LAB5*). By contrast, genes involved in drug transport (33 genes; e.g., *CDR1*, *CDR2*, *SNQ2* encoding ABC transporters, and *MRR1* multidrug resistance regulator 1 transcriptional factor), response to oxidative stress (17 genes; e.g., *CIP1*, *SOD1*, *SOD2*, *SOD6*, *PST1*), glutathione metabolism (16 genes; e.g., *TTR1*, *GST2*, *GPX1*), and fatty acid degradation (13 genes) were upregulated by the 200-µM HSL treatment (Table 1 and S2).

Based on transcriptomic data for 100-µM HSL-treated *C. albicans*, genes associated with the mitotic cell cycle (21 genes), sterol biosynthesis (8 genes; e.g., *ERG1*, *ERG3*), and cell cycle/morphological transition regulation (e.g., *CCN1*, *GIN4*, *HSL1* encoding protein kinases) were also downregulated, while fatty acid degradation (8 genes) was upregulated by the 100-µM HSL treatment (Table 1 and S2). Conversely, 100-µM HSL treatment resulted in the enrichment of upregulated RNA metabolic processes (99 genes) and ribosome biogenesis (73 genes) (Table 1 and S2).

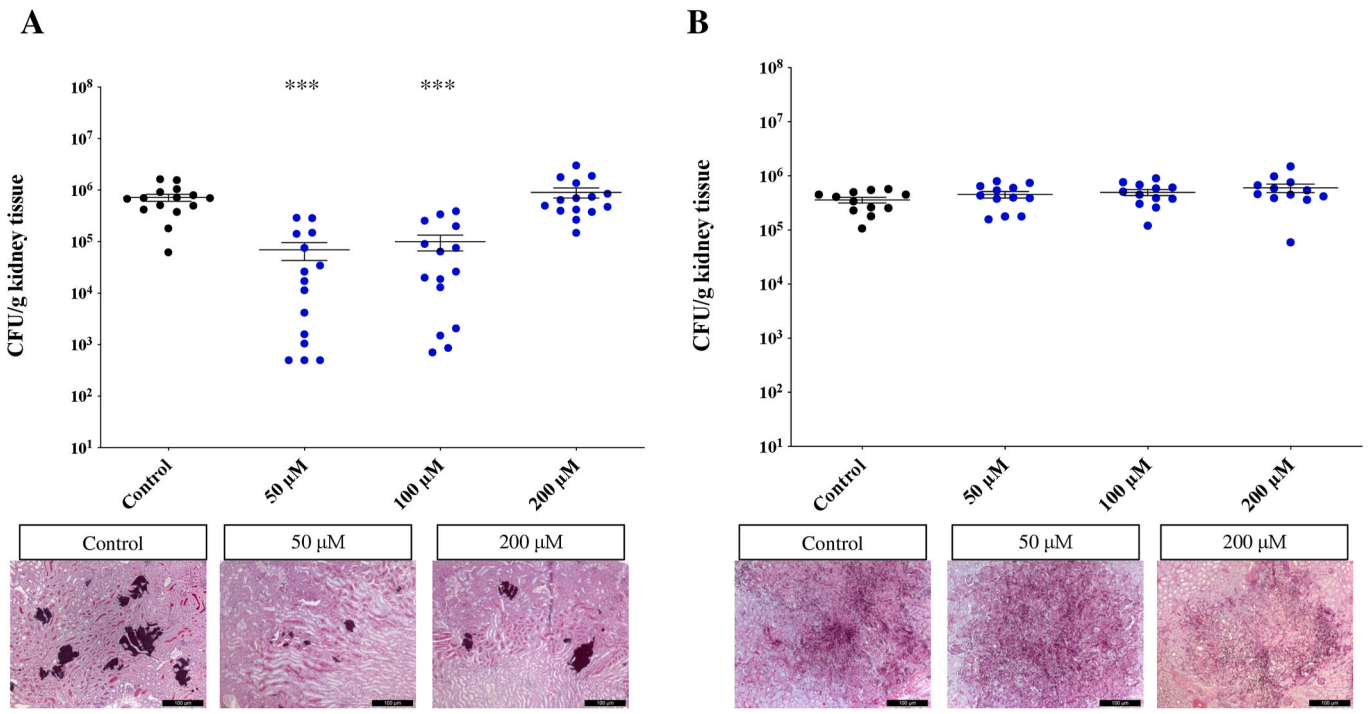

Fig. 3. The kidney burden of *Candida auris* (A) and *C. albicans* (B) in a systemically infected mouse model. The bars represent the means ± SD (standard deviation) of kidney tissue burdens of BALB/c mice. Significant differences between CFU numbers were determined based on comparison with the untreated controls. Levels of significant differences are indicated (***$p < 0.001$). Histological changes in kidney tissue from mice suffering from systemic candidiasis with or without 3-oxo-C12-homoserine lactone (HSL) treatment were examined by Periodic acid-Schiff staining.

3.5. Transcriptome response of *C. auris* to HSL

In total, 474 genes were differentially expressed by a ≥1.5-fold change following 200-μM HSL treatment compared with the untreated condition, including 306 upregulated and 168 downregulated genes (Fig. 4A). The transcriptional response of *C. auris* to 100-μM HSL treatment was relatively subtle, with only 67 upregulated and 111 downregulated genes compared with the untreated condition (Fig. 4A). We identified 45 overlapping upregulated and 25 overlapping downregulated genes between the 100- and 200-μM HSL treatments (Fig. 4C) and only one overlapping upregulated gene between the HSL-treated *C. albicans* and *C. auris* (Fig. 4D). The RNA-seq data showed a strong correlation with the RT-qPCR data for the selected 10 genes (Pearson's correlation coefficient: 0.92–0.94) (Table S1).

Our transcriptomic results reveal global gene expression changes in *C. auris* during the 200-μM HSL treatment. Upregulated genes were associated with processes such as transmembrane transport (34 genes; e.g., antifungal drug transporters *CDR1* and *CDR4* and phosphate transporter *PHO84*), peroxisome (21 genes), mitochondrion (40 genes), iron ion homeostasis (*FTH1*, *FRE9*, *HMX1*, four predicted heme-binding proteins, *RLI1*, ABC protein, *ALK2*, N-alkane inducible cytochrome P450, and *CDG1*, cysteine dioxygenase), and fatty acid degradation (22 genes) compared with the untreated condition (Table 1, Fig. 5A and B, Table S2).

Conversely, downregulated genes included those involved in transmembrane transport (36 genes; e.g., drug transporters *MLT1* and *B9J08_003832*, copper and zinc transporters *CTR1*, *ZRT2*, and *B9J08_003341*), iron ion homeostasis (*FRP1*, *FTR1*, *FTP1*, *PGA7*, and *B9J08_003002*), glutathione metabolism (5 genes; e.g., *GCS1*, *GLR1*, *APE2*, and *RNR3*), DNA replication (9 genes), antifungal resistance (*MRR1*), and long-chain fatty acid biosynthetic processes (*FAS1* and *FAS2*, fatty acid synthases) compared with the untreated control (Table 1, Fig. 5B–Table S2). Both 100- and 200-μM HSL exposures decreased the transcription of *B9J08_001458* (*SCF1*), which encodes a *C. auris*-specific surface colonisation factor, and increased the expression of genes related to the modified β-oxidation pathway via 3-hydroxypropionate (5 genes: *POX1-3*, *FOX2*, *CAT2*, *CRC1*, and *HPD1*) (Fig. 5A and B).

Based on transcriptomic data for 100-μM HSL-treated *C. auris*, genes related to zinc ion binding (10 genes; e.g., transcription factors *SFU1* and *CRZ2*, predicted Zn(II)2Cys6 transcription factors *ZCF4* and *SUT1*, and zinc-finger transcription factor *IRF1*) were enriched in the upregulated gene set. By contrast, genes associated with the pre-replicative complex (*MCM6* and *CDC6*), translation (25 genes), ribosome biogenesis (20 genes), sterol biosynthesis (*ERG2*, *ERG5*, and *ERG13*), and drug transport (*MDR1* and *ROA1*) were enriched in the downregulated gene set in the presence of 100-μM HSL (Table 1, Fig. 5A–Table S2).

3.6. HSL exposure significantly influences the intracellular iron and zinc metal contents of *C. auris* cells

HSL exposure caused significant transcriptional changes in metal-related genes in *C. auris*; however, these alterations did not immediately manifest phenotypically. The physiological changes were only observed after a 4-h treatment. Following 4 h of exposure to 100 and 200-μM HSL, the iron content of treated yeast cells decreased to 155.0 ± 30.6 and 117.5 ± 12.5 mg/kg, respectively, compared with controls (231.6 ± 6.7 mg/kg) ($p < 0.05$–0.001) (Fig. 6). Similarly, the zinc content decreased to 436.6 ± 54.4 and 326.4 ± 27.8 mg/kg for the 100- and 200-μM HSL treatments, respectively, compared with controls (612.1 ± 19.3 mg/kg) ($p < 0.05$–0.001). By contrast, the copper (11.7 ± 1.8 and 11.6 ± 2.3 mg/kg) and manganese (33.7 ± 3.5 and 29.6 ± 1.9 mg/kg) contents of 100 and 200-μM HSL-treated *C. auris* cells did not differ significantly from those of the untreated control cultures (9.7 ± 0.5 mg/kg for copper and 29.4 ± 0.9 mg/kg for manganese) ($p > 0.05$) (Fig. 6).

In the case of *C. albicans*, no significant changes in gene expression related to intracellular metal content were detected following exposure to 100 or 200-μM HSL at either 2 or 4 h. As a result, metal measurements were not performed for *C. albicans*.

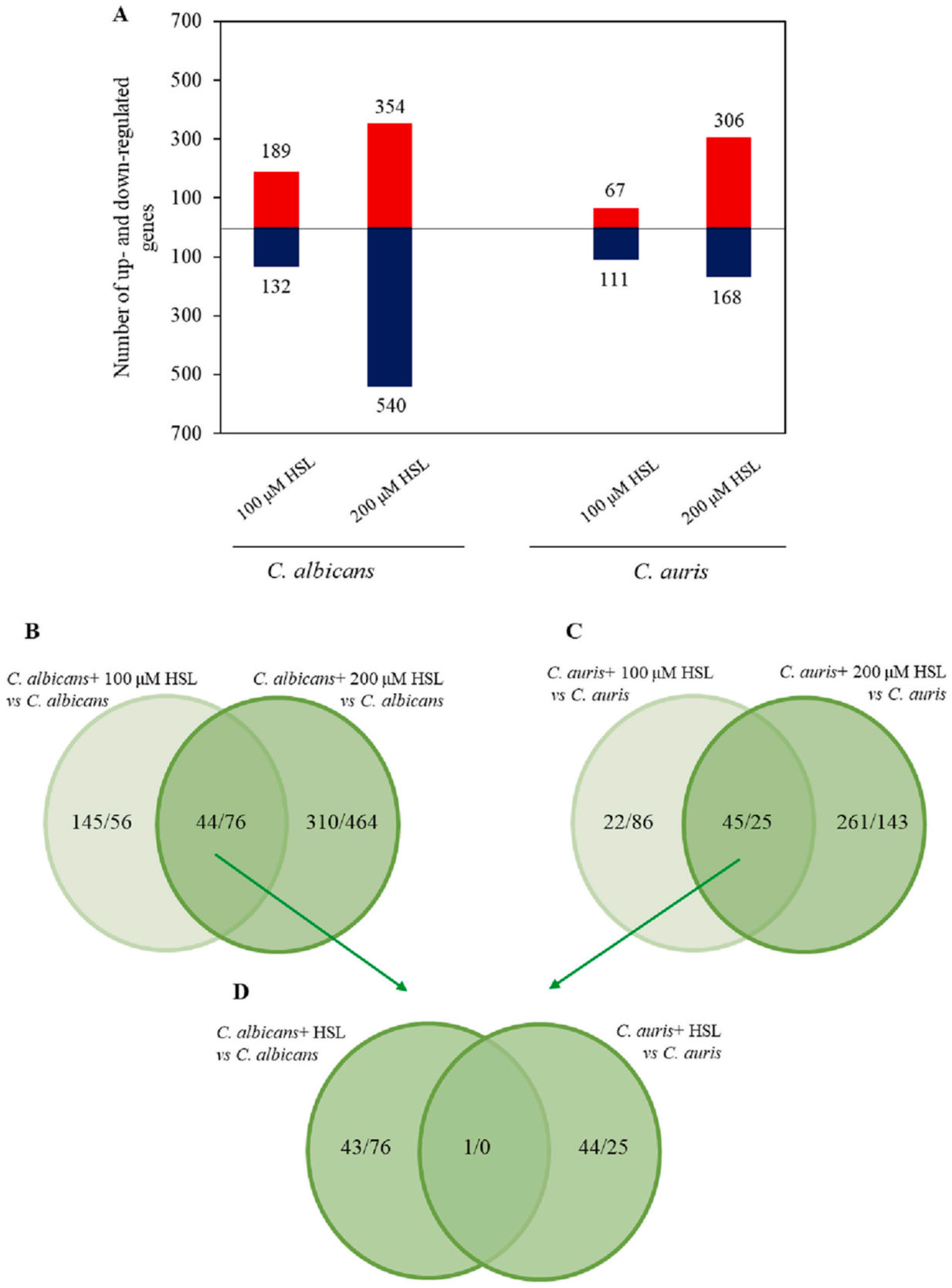

Fig. 4. Number of up and downregulated genes for *Candida auris* and *C. albicans*, respectively. Panel A shows the number of up- (red) and downregulated (blue) genes. Only the differentially expressed genes (DEGs; corrected *p* value of <0.05) exhibiting more than 1.5-fold increase or decrease (FC > 1.5, and FC < −1.5) in their transcription are shown. Panels B–D show the Venn-analysis of up- and downregulated genes in HSL treated *C. albicans* (B) and *C. auris* (C) strains as well as the overlapping up- and downregulated genes during *C. albicans* and *C. auris* responses to 100 and 200-µM HSL treatments (D). The number of upregulated/downregulated genes are presented. (For interpretation of the references to colour in this figure legend, the reader is referred to the Web version of this article.)

Table 1
Summary of gene enrichment analyses.

Significantly enriched gene groups	Number of up- and downregulated genes (with corrected *p* value) [a]			
	Candida albicans		*Candida auris*	
	100 μM HSL *vs* Cont	200 μM HSL *vs* Cont	100 μM HSL *vs* Cont	200 μM HSL *vs* Cont
Transmembrane transport		**46** (0.012)[c]	**15** (0.016)[c]	**34** (0.0005)[c] **36** (2.1×10^{-10})[c]
Drug transport		**33** (0.0001)[b]		
Glutathione metabolism		**16** (1.73×10^{-4})[c]		**5** (0.02)[c]
Response to oxidative stress		**17** (0.016)[c]		
Peroxisome			**11** (1.4×10^{-10})[c]	**21** (7.8×10^{-12})[c]
Mitotic cell cycle process	**21** (3.3×10^{-6})[c]	**54** (1.17×10^{-6})[c]		
DNA replication		**32** (2.34×10^{-7})[c]		**9** (0.006)[c]
RNA metabolic process	**99** (6.1×10^{-22})[c]	**139** (0.005)[c]		
Ribosome biogenesis	**73** (1.0×10^{-18})[b]	**136** (3.6×10^{-11})[c]	**20** (2.8×10^{-6})[c]	
Translation		**125** (2.7×10^{-15})[b]	**25** (4.5×10^{-17})[b]	
Mitochondrion				**40** (0.03)[c]
Iron ion transmembrane transport	**2** (0.012)[c]	**3** (0.028)[c]		**2** (0.022)[c]
Zinc ion transmembrane transport				**2** (0.005)[c]
Iron ion binding			**5** (0.003)[c]	**7** (0.008)[c]
Zinc ion binding			**10** (0.001)[c]	
Fatty acid biosynthetic process		**8** (0.01)[c]		**5** (0.013)[c]
Fatty acid degradation	**8** (0.0024)[c]	**13** (0.008)[c]	**5** (0.001)[c]	**22** (6.9×10^{-12})[c]
Sterol biosynthetic process	**8** (0.033)[c]	**32** (3.54×10^{-5})[c]	**3** (0.031)[c]	

a Bold numbers represent the up-regulated (red) or downregulated (blue) genes belonging to gene groups in comparisons where the enrichment was significant; *p* values are given in parentheses. Up- and downregulated genes were defined as differentially expressed genes (DEGs).
b Selected significant Gene Ontology (GO) terms ($p < 0.05$) were identified with the aid of *Candida* Genome Database Gene Ontology Term Finder (http://www.candidagenome.org/cgi-bin/GO/goTermFinder). The full list of the significantly enriched GO terms is available in Supplementary Table 2.
c The FungiDB platform (https://fungidb.org/fungidb/app/) with default settings was used for the characterisation of the up- and downregulated gene sets. The full list of the significantly enriched terms is available in Supplementary Table 2.

4. Discussion

The interaction between *P. aeruginosa* and *C. albicans* is frequently used to model fungal-bacterial cross-kingdom relationships, often characterised as competitive and antagonistic, at least under *in vitro* conditions. Based on extensive studies, *P. aeruginosa* inhibits *C. albicans* morphological transition from yeast to hyphae using secreted chemicals. Several studies suggest that *Pseudomonas* quorum sensing molecules – primarily HSL – are responsible for the signal-mediated communications between these two microorganisms [6,7,26–30]. However, observations derived from *C. albicans* cannot be directly extrapolated to *Pseudomonas*-non-albicans co-habitation [8–10]. For example, because of its effective skin and mucosal colonisation, *C. auris* coexists with various commensal Gram-negative microorganisms, including *P. aeruginosa*, yet our current knowledge is limited regarding this clinically relevant bacterial–fungal interaction [11,12].

In this context, we investigated how *C. auris* responds to the primary *P. aeruginosa* quorum-sensing molecule, HSL. Previous analytical studies using gas chromatography-mass spectrometry have shown that mature *P. aeruginosa* biofilms may contain >600-μM of HSL [14]. Furthermore, studies have shown that 200-μM of HSL inhibits hyphal growth in *C. albicans*, while concentrations exceeding 500-μM completely prevent fungal growth [14]. Therefore, the range of HSL concentrations tested on *C. auris* in this study (50–200-μM) is considered relevant to potential clinical scenarios. Our findings provide strong evidence that several responses to HSL are *C. auris*-specific, with only a few overlapping responses in direct comparison to *C. albicans*. It has been previously reported in *C. albicans* that the response to bacterial quorum-sensing molecules is mainly limited to compounds with a 12-carbon backbone, similar to its native quorum-sensing molecules, including sesquiterpene alcohol farnesol [31]. Thus, it is not surprising that the HSL responses observed in *C. auris* resemble the specific effects of farnesol, at least at a physiological level [10].

HSL-based interactions between prokaryotic and eukaryotic cells have been extensively studied over the past two decades. Hogan et al. [32] demonstrated that HSL not only inhibits *C. albicans* filamentation but also induces the reversion of *C. albicans* filaments back to yeast-form cells. Jarosz et al. [33] found that HSL plays a crucial role in the expression of *P. aeruginosa* adhesion proteins, which is essential for the adherence of *C. albicans* hyphae in a mixed *C. albicans–P. aeruginosa* population. Moreover, HSL has been reported to mediate Ca^{2+} dysregulation, mitochondrial dysfunction, and apoptosis in certain human cells, as well as disrupt the intestinal epithelial cell barrier by collapsing the extracellular matrix and tight junctions. These effects, however, are concentration-dependent and cell-line specific [19].

Our transcriptome analysis revealed that HSL significantly affected several multidrug transporter-related genes in both species tested, regardless of the concentration. Bandara et al. [34] reported that HSL

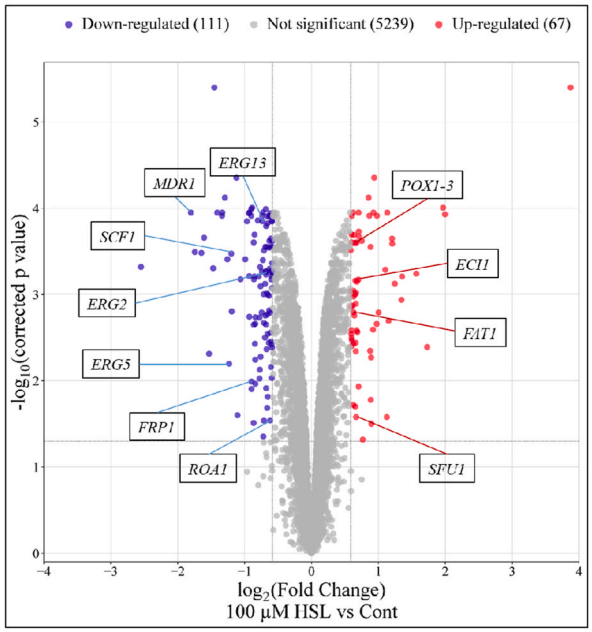

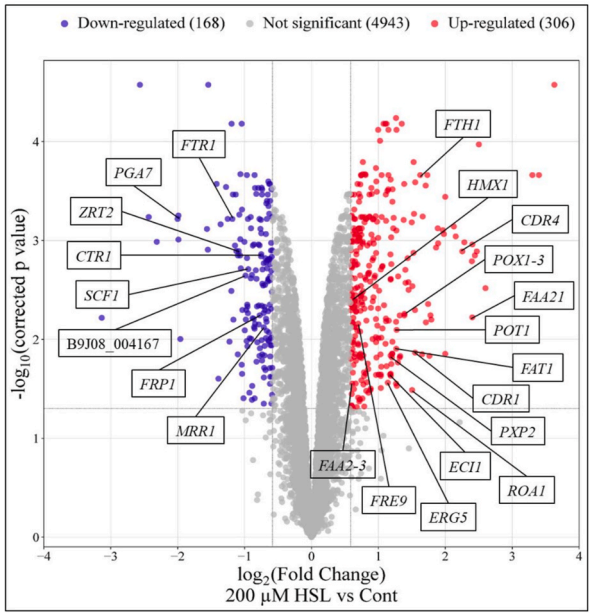

Fig. 5. Overview of transcriptional changes induced by 100 (A) and 200-µM (B) 3-oxo-C12-homoserine lactone (HSL) in *Candida auris*. Up-regulated (red) and down-regulated (blue) genes were defined as differentially expressed genes (corrected *p* value of,0.05), with more than a 1.5-fold increase or decrease in their transcription (HSL treated versus untreated). On the sides of the volcano plot are representative genes up-regulated or down-regulated by HSL treatment. The data set is available in Table S2 in the supplemental material. (For interpretation of the references to colour in this figure legend, the reader is referred to the Web version of this article.)

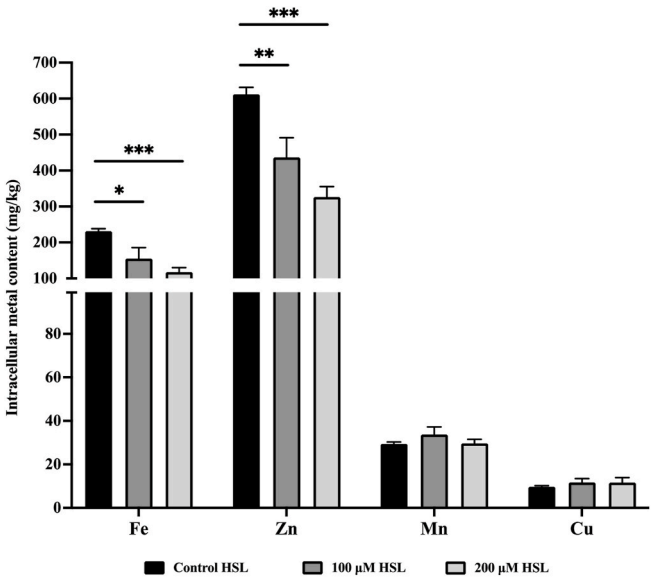

Fig. 6. Intracellular iron (Fe), zinc (Zn), manganese (Mn) and copper (Cu) content (mg/kg) following 100 and 200-µM compared to untreated control cells in *Candida auris*. Levels of significant differences are indicated (*$p <$ 0.05, **$p < 0.01$, ***$p < 0.001$).

stimulates the multidrug efflux activity of *C. albicans* by modulating the transcription of genes such as *CDR1*, *CDR2*, and *MDR1* and influences its response to fluconazole. In *C. albicans*, we observed that both *CDR1* and *CDR2* were upregulated by 200-µM HSL, with levels significantly higher than those produced by the 100-µM treatment. For *C. auris*, *CDR1* and *CDR4* were also upregulated by 200-µM HSL, with a significant difference in transcription levels between the 100- and 200-µM treatments. Previous studies have also reported the evidence with regard to upregulation of efflux pumps belonging to ABC superfamily by C12 compounds as farnesol or HSL against *C. albicans* or *C. auris* without upregulation of MDR genes [10,35]. In *C. albicans CDR1* is a gene encoding for and ABC efflux pump, known for its role in azole resistance. A gene homologous to *CDR1* was found in *C. auris*. Rybak et al. showed that deletion of this gene could increase susceptibility of resistant strains from 64 -to 128-fold [36]. Interestingly, 100-µM HSL caused significant downregulation of the *ROA1* and *MDR1* ABC transporter genes in *C. auris*, as well as *MRR1*, which plays a major role in resistance against azole antifungals [37]. It is also noteworthy, that our physiological data support the hypothesis that HSL may be a potential substrate for this overexpressed transport proteins to protect the fungal cells against harmful effect of HSL [10].

Concerning membrane ergosterol content, HSL had a more pronounced negative effect on ergosterol synthesis in *C. albicans* than in *C. auris*. Bandara et al. [34] suggested that HSL might confer protection to neighbouring *Candida* cells against fluconazole, enhancing their survival in hostile polymicrobial infections. In this study, several *ERG* genes were downregulated in *C. albicans* upon HSL exposure, with a more substantial impact observed at 200-µM than at 100-µM. Specifically, *ERG3*, *ERG6*, and *ERG11* were significantly downregulated, potentially affecting fluconazole susceptibility [34]. Notably, the conditions used by Bandara et al. [34] differed from our study, which could explain the variations in our findings. For *C. auris*, only *ERG2*, *ERG5*, and *ERG13* were downregulated by 100-µM HSL, potentially increasing susceptibility to azoles [38]. The downregulation of these three *ERG* genes has pivotal role in amphotericin B susceptibility in *C. auris* as published previously Frías-De-León et al. [39].

Our adhesion-based experiments showed that HSL treatment significantly influenced the morphology and metabolic activity of adhered cells. For *C. auris*, large cell aggregates were observed, resembling morphological changes induced by amphotericin B or echinocandin [17]. The antifungal-induced aggregation is the result of a cell separation defect as published previously [40]. Pelletier et al. showed that antifungal treatment causes a cell separation defect which leads to the formation of cell clusters. This phenotype is independent of the ability to aggregate in response to the culturing medium, which has been assumed to be the typical aggregation phenotype [40]. Other potential explanation may be the divalent cation depletion induced aggregation. Holmes

et al. reported that the addition of divalent cations (Ca^{2+}, Zn^{2+}, Cu^{2+}, Fe^{2+}, Mg^{2+}) caused immediate aggregation of *Candida* cell culture [41]. These findings suggest that divalent cation crossbridging between opposing anionic sites and protein interactions may act synergistically to promote aggregation of *Candida* cells [41]. In our study, we observed significant iron and zinc intracellular ion decrease and simultaneously transporter pumps overexpression which may lead to the increased concentration of divalent cations in culturing medium.

Additionally, the transcription of the surface colonisation factor *SCF1* was downregulated following HSL treatment. *SCF1* is crucial for attachment to abiotic surfaces, skin, and biofilm formation in *C. auris*, and its downregulation may explain the reduced adhesion and biofilm formation observed in HSL-treated cells [42].

Although the hypha formation of *C. albicans* was not significantly inhibited by HSL during the observation period, its morphology and arrangement were significantly altered compared with untreated control cells. Similar effects were observed by Hogan et al., where the HSL-induced effect was very pronounced after 6 h of incubation [32]. In their experiments, *C. albicans* growth rate was indistinguishable from that of *C. albicans* in medium alone or containing an equivalent volume of solvent in the presence of 500-μM HSL [32]. Previous studies have reported that HSL concentrations between 100 and 200-μM completely suppressed *HWP1* expression, thereby influencing the hyphae-forming ability of *C. albicans* [43]. In another analysis, both the yeast-hyphal transition and biofilm-forming ability were impaired by *Pseudomonas* supernatants containing HSL [43]. A comprehensive study examining wild-type and 63 mutant strains exposed to supernatant from wild-type and HSL-negative strains of *P. aeruginosa* revealed an HSL-dependent negative effect on *C. albicans* morphology [44].

In addition to these morphological changes, we also examined the metabolic activity of adhered cells. Regarding the transcription profiles of metabolism-related genes, marked differences were detected between *C. albicans* and *C. auris* following HSL exposure, particularly in the fatty acid oxidation pathway. In *C. auris*, a similar transcription profile was observed compared to farnesol-exposed *C. auris* cells, as previously reported [10]. More than 60 % of fatty acid oxidation-related genes were significantly upregulated following HSL exposure; moreover, additional genes (e.g., *FAA21*, *POT1*, *POX1-3*) showed significant differences in their transcription levels between 100 and 200-μM treatments. By contrast, only 20 % of these genes were upregulated in *C. albicans*, and this effect was exclusively observed following the 100-μM exposure. Jakab et al. observed similar metabolic pattern in *C. auris* following farnesol exposure [10]. The increased usage of fatty acids and total or partly elimination of membrane lipid provides a higher metabolic flux, needed for the maintenance of membrane fluidity [45]. This process may be necessary due to the downregulation of ergosterol genes. Our transcriptome analysis revealed that HSL treatment significantly impacts the modified β-oxidation pathway in *C. auris* via 3-hydroxypropionate [46]. The modified β-oxidation pathway could serve as a novel target for antifungal compounds, as detoxification of propionyl-CoA is crucial to maintaining normal cellular functions. Propionyl-CoA is a metabolic intermediate derived from the degradation of propionate, odd-chain fatty acids, and some amino acids. A third pathway for the degradation of propionyl-CoA has been described, involving a modified β-oxidation process characterised by the formation of β-hydroxypropionate [46].

To further investigate the virulence-related effects of HSL, an immunocompromised systemic mouse model was used. Interestingly, HSL treatments had no effect on *C. albicans* virulence properties *in vivo*, as confirmed by fungal burden results and histological examinations. By contrast, a surprising susceptibility profile was observed for *C. auris in vivo*. Lower HSL treatment concentrations (50–100-μM) significantly decreased the number of viable fungal cells in the kidneys. Additionally, the size of fungal lesions was smaller and less extensive compared to both untreated control cells and cells treated with a higher HSL concentration (200-μM). Similar results were obtained in case of farnesol treatment against *C. auris* and *C. albicans*. Seventy-five-μM farnesol treatment arm reduced the fungal kidney burden. In case of *C. albicans*, farnesol treatment produced statistically comparable kidney fungal burdens compared to untreated control [8]. Huang et al. reported that 200-μM HSL treatment significantly decreased bacterial burden and increased the survival rate in Kunming mice against *Trueperella pyogenes* challenge [47]. Additionally, HSL had a remarkable immunomodulator effect because it promoted the secretion of IL-1β, IL-6, IL-8 and TNF-α; furthermore, it significantly reduced the transcription level of virulence genes of *T. pyogenes* [47].

Among the species and HSL concentrations studied, fatty acid oxidation was the only pathway that showed a significant difference in gene transcription levels between species and between HSL concentrations within each *Candida* species. Fatty acid oxidation is closely linked to *Candida* virulence due to its roles in metabolic adaptation, energy production, immune evasion, and morphogenesis. Previous studies have suggested that the ability of *C. albicans* to convert fatty acids into glucose might contribute to its virulence *in vivo* [48–50]. However, other studies have indicated that fatty acid metabolism via β-oxidation appears to be dispensable for virulence in *C. albicans* [51].

Beyond the observed differences in fungal metabolism, HSL treatment significantly decreased intracellular iron and zinc content in *C. auris*, contributing to the previously discussed beta-oxidation-based anti-virulence effect at 50 and 100-μM treatments [52,53]. Both iron and zinc are major modulators of virulence in various human fungal pathogens, including *Candida* species. An imbalance in these metal ions, whether in excess or deficiency, has been associated with reduced *in vivo* virulence [52,53]. Interestingly, a similar altered metabolic state and negatively affected ion milieu were observed with farnesol treatment in *C. auris*, which was also linked to impaired virulence *in vivo* [10]. These findings further support the hypothesis that 12-carbon backbone-based quorum-sensing molecules may universally affect certain aspects of fungal physiology, such as fatty acid oxidation, virulence properties, and intracellular metal content, at least in *C. auris*.

5. Conclusion

In summary, our data highlight that HSL not only inhibits specific *C. albicans* processes but also negatively influences several physiological properties in *C. auris*. Similar to the C12 compound farnesol, HSL reduces several fungal survival strategies. We demonstrated its adhesion-reducing effect on *C. auris* cells, its role in decreasing iron and zinc contents, and its modulation of *C. auris* metabolism toward beta-oxidation, which may be associated with reduced *in vivo* virulence at lower HSL concentrations. Further detailed investigations into HSL-induced plasma membrane composition, biofilm-forming properties, and fungal metabolism are necessary. The obtained findings on *C. auris* do not provide clear evidence that HSL mediated effects have any favourable consequences in terms of *P. aeruginosa-C. auris* co-colonisation and/or co-infections. Primarily, the HSL induced negative, inhibitory effects are predominant similar to other quorum-sensing compounds with a 12-carbon backbone. Therefore, future studies should focus on direct *Candida–Pseudomonas* interactions in polymicrobial infections, as these interactions may have distinct effects compared to those mediated solely by HSL.

CRediT authorship contribution statement

Fruzsina Kovács: Writing – original draft, Visualization, Project administration, Methodology, Investigation, Conceptualization. **Ágnes Jakab:** Writing – original draft, Methodology, Investigation. **Noémi Balla:** Methodology, Investigation. **Zoltán Tóth:** Methodology, Investigation. **Dávid Balázsi:** Methodology, Investigation. **Lajos Forgács:** Methodology, Investigation. **Andrea Harmath:** Methodology, Investigation. **Aliz Bozó:** Methodology, Investigation. **Ágota Ragyák:** Methodology, Investigation. **László Majoros:** Writing – review & editing,

Data curation. **Renátó Kovács:** Writing – review & editing, Writing – original draft, Visualization, Validation, Supervision, Software, Project administration, Methodology, Investigation, Funding acquisition, Formal analysis, Data curation, Conceptualization.

Data availability

The RNA sequencing data were deposited into the Gene Expression Omnibus database (GEO; http://www.ncbi.nlm.nih.gov/geo/) under GEO series accession number GSE271513.

Funding

R. Kovács was supported by the Janos Bolyai Research Scholarship of the Hungarian Academy of Sciences (BO/00127/21/8). This research was supported by the Hungarian National Research, Development and Innovation Office (NKFIH FK138462).

Declaration of competing interest

The authors declare that they have no known competing financial interests or personal relationships that could have appeared to influence the work reported in this paper.

Acknowledgements

The authors thank Andrew M Borman for his generous gifts of *Candida auris* isolates.

Appendix A. Supplementary data

Supplementary data to this article can be found online at https://doi.org/10.1016/j.bioflm.2025.100259.

Data availability

The RNA sequencing data were deposited into the Gene Expression Omnibus database (GEO; http://www.ncbi.nlm.nih.gov/geo/) under GEO series accession number GSE271513.

References

[1] Rafat Z, Ramandi A, Khaki PA, Ansari S, Ghaderkhani S, Haidar H, Tajari F, Roostaei D, Ghazvini RD, Hashemi SJ, Abdollahi A, Kamali Sarvestani H. Fungal and bacterial co-infections of the respiratory tract among patients with COVID-19 hospitalized in intensive care units. Gene Rep 2022 Jun;27:101588. https://doi.org/10.1016/j.genrep.2022.101588.

[2] Zhong L, Dong Z, Liu F, Li H, Tang K, Zheng C, Wang L, Zhang K, Cai J, Zhou H, Cui W, Gao Y, Zhang G. Incidence, clinical characteristics, risk factors and outcomes of patients with mixed Candida/bacterial bloodstream infections: a retrospective study. Ann Clin Microbiol Antimicrob 2022 Nov 1;21(1):45. https://doi.org/10.1186/s12941-022-00538-y.

[3] MacAlpine J, Robbins N, Cowen LE. Bacterial-fungal interactions and their impact on microbial pathogenesis. Mol Ecol 2023 May;32(10):2565–81. https://doi.org/10.1111/mec.16411.

[4] De Sordi L, Mühlschlegel FA. Quorum sensing and fungal-bacterial interactions in Candida albicans: a communicative network regulating microbial coexistence and virulence. FEMS Yeast Res 2009 Oct;9(7):990–9. https://doi.org/10.1111/j.1567-1364.2009.00573.x.

[5] Delago A, Gregor R, Dubinsky L, Dandela R, Hendler A, Krief P, Rayo J, Aharoni A, Meijler MM. A bacterial quorum sensing molecule elicits a general stress response in *Saccharomyces cerevisiae*. Front Microbiol 2021 Sep 16;12:632658. https://doi.org/10.3389/fmicb.2021.632658.

[6] Fourie R, Pohl CH. *Beyond* antagonism: the interaction between *Candida* species and *Pseudomonas aeruginosa*. J Fungi (Basel) 2019 Apr 19;5(2):34. https://doi.org/10.3390/jof5020034.

[7] Miranda SW, Asfahl KL, Dandekar AA, Greenberg EP. Pseudomonas aeruginosa quorum sensing. Adv Exp Med Biol 2022;1386:95–115. https://doi.org/10.1007/978-3-031-08491-1_4.

[8] Nagy F, Vitális E, Jakab Á, Borman AM, Forgács L, Tóth Z, Majoros L, Kovács R. *In vitro* and *in vivo* effect of exogenous farnesol exposure against *Candida auris*. Front Microbiol 2020 May 20;11:957. https://doi.org/10.3389/fmicb.2020.00957.

[9] Jakab Á, Tóth Z, Nagy F, Nemes D, Bácskay I, Kardos G, Emri T, Pócsi I, Majoros L, Kovács R. Physiological and transcriptional responses of Candida parapsilosis to exogenous tyrosol. Appl Environ Microbiol 2019 Oct 1;85(20):e01388. https://doi.org/10.1128/AEM.01388-19. 19.

[10] Jakab Á, Balla N, Ragyák Á, Nagy F, Kovács F, Sajtos Z, Tóth Z, Borman AM, Pócsi I, Baranyai E, Majoros L, Kovács R. Transcriptional profiling of the Candida auris response to exogenous farnesol exposure. mSphere 2021 Oct 27;6(5):e0071021. https://doi.org/10.1128/mSphere.00710-21.

[11] Sexton DJ, Bentz ML, Welsh RM, Derado G, Furin W, Rose LJ, Noble-Wang J, Pacilli M, McPherson TD, Black S, Kemble SK, Herzegh O, Ahmad A, Forsberg K, Jackson B, Litvintseva AP. Positive correlation between Candida auris skin-colonization burden and environmental contamination at a ventilator-capable skilled nursing facility in chicago. Clin Infect Dis 2021 Oct 5;73(7):1142–8. https://doi.org/10.1093/cid/ciab327.

[12] Proctor DM, Dangana T, Sexton DJ, Fukuda C, Yelin RD, Stanley M, Bell PB, Baskaran S, Deming C, Chen Q, Conlan S, Park M, Welsh RM, Vallabhaneni S, Chiller T, Forsberg K, Black SR, Pacilli M, Kong HH, Lin MY, Schoeny ME, Litvintseva AP, Segre JA, Hayden MK, NISC Comparative Sequencing Program. Integrated genomic, epidemiologic investigation of Candida auris skin colonization in a skilled nursing facility. Nat Med 2021 Aug;27(8):1401–9. https://doi.org/10.1038/s41591-021-01383-w.

[13] Tharp B, Zheng R, Bryak G, Litvintseva AP, Hayden MK, Chowdhary A, Thangamani S. Role of microbiota in the skin colonization of Candida auris. mSphere 2023 Feb 21;8(1):e0062322. https://doi.org/10.1128/msphere.00623-22.

[14] Charlton TS, de Nys R, Netting A, Kumar N, Hentzer M, Givskov M, Kjelleberg S. A novel and sensitive method for the quantification of N-3-oxoacyl homoserine lactones using gas chromatography-mass spectrometry: application to a model bacterial biofilm. Environ Microbiol 2000 Oct;2(5):530–41. https://doi.org/10.1046/j.1462-2920.2000.00136.x.

[15] Jakab Á, Kovács F, Balla N, Tóth Z, Ragyák Á, Sajtos Z, Csillag K, Nagy-Köteles C, Nemes D, Bácskay I, Pócsi I, Majoros L, Kovács ÁT, Kovács R. Physiological and transcriptional profiling of surfactin exerted antifungal effect against Candida albicans. Biomed Pharmacother 2022 Aug;152:113220. https://doi.org/10.1016/j.biopha.2022.113220.

[16] Hawser S. Comparisons of the susceptibilities of planktonic and adherent Candida albicans to antifungal agents: a modified XTT tetrazolium assay using synchronised C. albicans cells. J Med Vet Mycol 1996 Mar-Apr;34(2):149–52.

[17] Papp Z, Borman AM, Forgács L, Kovács R, Tóth Z, Chun-Ju C, Kardos G, Juhász B, Szilvássy J, Majoros L. Unpredictable in vitro killing activity of amphotericin B against four *Candida auris* clades. Pathogens 2021 Aug 6;10(8):990. https://doi.org/10.3390/pathogens10080990.

[18] Lynch DP, Gibson DK. The use of Calcofluor white in the histopathologic diagnosis of oral candidiasis. Oral Surg Oral Med Oral Pathol 1987 Jun;63(6):698–703. https://doi.org/10.1016/0030-4220(87)90373-2.

[19] Neely AM, Zhao G, Schwarzer C, Stivers NS, Whitt AG, Meng S, Burlison JA, Machen TE, Li C. N-(3-Oxo-acyl)-homoserine lactone induces apoptosis primarily through a mitochondrial pathway in fibroblasts. Cell Microbiol 2018 Jan;20(1). https://doi.org/10.1111/cmi.12787. 10.1111/cmi.12787.

[20] Zhao G, Neely AM, Schwarzer C, Lu H, Whitt AG, Stivers NS, Burlison JA, White C, Machen TE, Li C. N-(3-oxo-acyl) homoserine lactone inhibits tumor growth independent of Bcl-2 proteins. Oncotarget 2016 Feb 2;7:5924–42. https://doi.org/10.18632/oncotarget.6827.

[21] Cheng W, Wang Z, Xiong Y, Wu Z, Tan X, Yang Y, Zhang H, Zhu X, Wei H, Tao S. N-(3-oxododecanoyl)-homoserine lactone disrupts intestinal barrier and induces systemic inflammation through perturbing gut microbiome in mice. Sci Total Environ 2021 Jul 15;778:146347. https://doi.org/10.1016/j.scitotenv.2021.146347.

[22] Tao S, Luo Y, He Bin, Liu J, Qian X, Ni Y, Zhao R. Paraoxonase 2 modulates a proapoptotic function in LS174T cells in response to quorum sensing molecule N-(3-oxododecanoyl)-L-homoserine lactone. Sci Rep 2016 Jul 1;6:28778. https://doi.org/10.1038/srep28778.

[23] Pupim ACE, Campois TG, Araújo EJA, Svidizinski TIE, Felipe I. Infection and tissue repair of experimental cutaneous candidiasis in diabetic mice. J Med Microbiol 2017 Jun;66(6):808–15. https://doi.org/10.1099/jmm.0.000496.

[24] Jakab Á, Kovács F, Balla N, Nagy-Köteles C, Ragyák Á, Nagy F, Borman AM, Majoros L, Kovács R. Comparative transcriptional analysis of *Candida auris*biofilms following farnesol and tyrosol treatment. Microbiol Spectr 2024 Apr 2;12(4):e0227823. https://doi.org/10.1128/spectrum.02278-23.

[25] Chomczynski P. A reagent for the single-step simultaneous isolation of RNA, DNA and proteins from cell and tissue samples. Biotechniques 1993 Sep;15(3):536–7. 532-4.

[26] Grainha T, Jorge P, Alves D, Lopes SP, Pereira MO. Unraveling *Pseudomonas aeruginosa* and *Candida albicans* communication in coinfection scenarios: insights through network analysis. Front Cell Infect Microbiol 2020 Nov 11;10:550505. https://doi.org/10.3389/fcimb.2020.550505.

[27] Morales DK, Grahl N, Okegbe C, Dietrich LE, Jacobs NJ, Hogan DA. Control of Candida albicans metabolism and biofilm formation by Pseudomonas aeruginosa phenazines. mBio 2013 Jan 29;4(1):e00526. https://doi.org/10.1128/mBio.00526-12. 12.

[28] Gibson J, Sood A, Hogan DA. Pseudomonas aeruginosa-Candida albicans interactions: localization and fungal toxicity of a phenazine derivative. Appl Environ Microbiol 2009 Jan;75(2):504–13. https://doi.org/10.1128/AEM.01037-08.

[29] Abd El-Baky RM, Mandour SA, Ahmed EF, Hashem ZS, Sandle T, Mohamed DS. Virulence profiles of some Pseudomonas aeruginosa clinical isolates and their

association with the suppression of Candida growth in polymicrobial infections. PLoS One 2020 Dec 8;15(12):e0243418. https://doi.org/10.1371/journal.pone.0243418.
[30] De Sordi L, Mühlschlegel FA. Quorum sensing and fungal-bacterial interactions in Candida albicans: a communicative network regulating microbial coexistence and virulence. FEMS Yeast Res 2009 Oct;9(7):990–9. https://doi.org/10.1111/j.1567-1364.2009.00573.x.
[31] Shchepin R, Hornby JM, Burger E, Niessen T, Dussault P, Nickerson KW. Quorum sensing in Candida albicans: probing farnesol's mode of action with 40 natural and synthetic farnesol analogs. Chem Biol 2003 Aug;10(8):743–50. https://doi.org/10.1016/s1074-5521(03)00158-3.
[32] Hogan DA, Vik A, Kolter R. A Pseudomonas aeruginosa quorum-sensing molecule influences Candida albicans morphology. Mol Microbiol 2004 Dec;54(5):1212–23. https://doi.org/10.1111/j.1365-2958.2004.04349.x.
[33] Jarosz LM, Ovchinnikova ES, Meijler MM, Krom BP. Microbial spy games and host response: roles of a Pseudomonas aeruginosa small molecule in communication with other species. PLoS Pathog 2011 Nov;7(11):e1002312. https://doi.org/10.1371/journal.ppat.1002312.
[34] Bandara HMHN, Wood DLA, Vanwonterghem I, Hugenholtz P, Cheung BPK, Samaranayake LP. Fluconazole resistance in Candida albicans is induced by Pseudomonas aeruginosa quorum sensing. Sci Rep 2020 May 8;10(1):7769. https://doi.org/10.1038/s41598-020-64761-3.
[35] Sharma M, Prasad R. The quorum-sensing molecule farnesol is a modulator of drug efflux mediated by ABC multidrug transporters and synergizes with drugs in Candida albicans. Antimicrob Agents Chemother 2011 Oct;55(10):4834–43. https://doi.org/10.1128/AAC.00344-11.
[36] Rybak JM, Doorley LA, Nishimoto AT, Barker KS, Palmer GE, Rogers PD. Abrogation of triazole resistance upon deletion of *CDR1* in a clinical isolate of *Candida auris*. Antimicrob Agents Chemother 2019 Mar 27;63(4):e00057. https://doi.org/10.1128/AAC.00057-19. 19.
[37] Biermann AR, Hogan DA. Transcriptional response of Candida auris to the Mrr1 inducers methylglyoxal and benomyl. mSphere 2022 Jun 29;7(3):e0012422. https://doi.org/10.1128/msphere.00124-22.
[38] Zamith-Miranda D, Heyman HM, Cleare LG, Couvillion SP, Clair GC, Bredeweg EL, Gacser A, Nimrichter L, Nakayasu ES, Nosanchuk JD. Multi-omics signature of *Candida auris*, an emerging and multidrug-resistant pathogen. mSystems 2019 Jun 11;4(4):e00257. https://doi.org/10.1128/mSystems.00257-19. 19.
[39] Frías-De-León MG, Hernández-Castro R, Vite-Garín T, Arenas R, Bonifaz A, Castañón-Olivares L, Acosta-Altamirano G, Martínez-Herrera E. Antifungal resistance in *Candida auris*: molecular determinants. Antibiotics (Basel) 2020 Sep 2;9(9):568. https://doi.org/10.3390/antibiotics9090568.
[40] Pelletier C, Shaw S, Alsayegh S, Brown AJP, Lorenz A. Candida auris undergoes adhesin-dependent and -independent cellular aggregation. PLoS Pathog 2024 Mar 11;20(3):e1012076. https://doi.org/10.1371/journal.ppat.1012076.
[41] Holmes AR, Cannon RD, Shepherd MG. Mechanisms of aggregation accompanying morphogenesis in Candida albicans. Oral Microbiol Immunol 1992 Feb;7(1):32–7. https://doi.org/10.1111/j.1399-302x.1992.tb00017.x.
[42] Santana DJ, Anku JAE, Zhao G, Zarnowski R, Johnson CJ, Hautau H, Visser ND, Ibrahim AS, Andes D, Nett JE, Singh S, O'Meara TR. A *Candida auris*-specific adhesin, Scf1, governs surface association, colonization, and virulence. Science 2023 Sep 29;381(6665):1461–7. https://doi.org/10.1126/science.adf8972.
[43] Hogan DA, Sundstrom P. The Ras/cAMP/PKA signaling pathway and virulence in Candida albicans. Future Microbiol 2009 Dec;4(10):1263–70. https://doi.org/10.2217/fmb.09.106.
[44] Konstantinidou N, Morrissey JP. Co-occurrence of filamentation defects and impaired biofilms in Candida albicans protein kinase mutants. FEMS Yeast Res 2015 Dec;15(8):fov092. https://doi.org/10.1093/femsyr/fov092.
[45] Fradin C, Abu-Arish A, Granek R, Elbaum M. Fluorescence correlation spectroscopy close to a fluctuating membrane. Biophys J 2003 Mar;84(3):2005–20. https://doi.org/10.1016/S0006-3495(03)75009-7.
[46] Otzen C, Bardl B, Jacobsen ID, Nett M, Brock M. Candida albicans utilizes a modified β-oxidation pathway for the degradation of toxic propionyl-CoA. J Biol Chem 2014 Mar 21;289(12):8151–69. https://doi.org/10.1074/jbc.M113.517672.
[47] Huang T, Song X, Zhao K, Jing J, Shen Y, Zhang X, Yue B. Quorum-sensing molecules N-acyl homoserine lactones inhibit Trueperella pyogenes infection in mouse model. Vet Microbiol 2018 Jan;213:89–94. https://doi.org/10.1016/j.vetmic.2017.11.029.
[48] Lorenz MC, Bender JA, Fink GR. Transcriptional response of Candida albicans upon internalization by macrophages. Eukaryot Cell 2004 Oct;3(5):1076–87. https://doi.org/10.1128/EC.3.5.1076-1087.2004.
[49] Lorenz MC, Fink GR. The glyoxylate cycle is required for fungal virulence. Nature 2001 Jul 5;412(6842):83–6. https://doi.org/10.1038/35083594.
[50] Prigneau O, Porta A, Poudrier JA, Colonna-Romano S, Noël T, Maresca B. Genes involved in beta-oxidation, energy metabolism and glyoxylate cycle are induced by Candida albicans during macrophage infection. Yeast 2003 Jun;20(8):723–30. https://doi.org/10.1002/yea.998.
[51] Piekarska K, Mol E, van den Berg M, Hardy G, van den Burg J, van Roermund C, MacCallum D, Odds F, Distel B. Peroxisomal fatty acid beta-oxidation is not essential for virulence of Candida albicans. Eukaryot Cell 2006 Nov;5(11):1847–56. https://doi.org/10.1128/EC.00093-06.
[52] Ballou ER, Wilson D. The roles of zinc and copper sensing in fungal pathogenesis. Curr Opin Microbiol 2016 Aug;32:128–34. https://doi.org/10.1016/j.mib.2016.05.013.
[53] Gerwien F, Skrahina V, Kasper L, Hube B, Brunke S. Metals in fungal virulence. FEMS Microbiol Rev 2018 Jan 1;42(1):fux050. https://doi.org/10.1093/femsre/fux050.